Polymer 53 (2012) 1593–1601

Contents lists available at SciVerse ScienceDirect

Polymer

journal homepage: www.elsevier.com/locate/polymer

Real time synchrotron SAXS and WAXS investigations on temperature related deformation and transitions of β-iPP with uniaxial stretching

Ziwei Cai [a], Yao Zhang [a], Jingqing Li [a], Feifei Xue [a], Yingrui Shang [a], Xuehao He [b], Jiachun Feng [c], Zhonghua Wu [d], Shichun Jiang [a,*]

[a] School of Materials Science and Engineering, Tianjin University, Tianjin 300072, PR China
[b] Department of Chemistry, School of Science, Tianjin University, Tianjin 300072, PR China
[c] Key Laboratory of Molecular Engineering of Polymers of Ministry of Education, Department of Macromolecular Science and Laboratory of Advanced Materials, Fudan University, Shanghai 200433, PR China
[d] Beijing Synchrotron Radiation Laboratory, Institute of High Energy Physics, Chinese Academy of Sciences, Beijing 100039, PR China

ARTICLE INFO

Article history:
Received 18 October 2011
Received in revised form
9 January 2012
Accepted 7 February 2012
Available online 13 February 2012

Keywords:
β PP deformation
Real time X-ray scattering
Auxetical behavior

ABSTRACT

In-situ synchrotron small-angle X-ray scattering (SAXS) and wide-angle X-ray scattering (WAXS) were carried out to investigate the uniaxial drawing-induced deformation and structure transitions of β form isotactic polypropylene (iPP) at varying temperatures (30 °C, 60 °C, 80 °C, 100 °C and 120 °C). The WAXS results indicated that the initial strain for the strain-induced β–α transformation decreases with the tensile temperature according to the engineering stress–strain curves. The SAXS data showed that the long period increased along the direction perpendicular to the tensile force and changed little along the tensile direction with increasing strain in the elastic deformation stage before the yield point. The analysis of the obtained scattering results indicated that the angle between parent and daughter lamella rotates from initial 40° or 140° to close to 90° accounts for the lateral expansion of the samples with tension, which matches the essential auxetical behavior. A structure deformation and transition mechanism was proposed for β form iPP with uniaxial drawing. The initialization of the crystalline structure transition is after the yield point, then the mechanical loading-induced β–α transition seems to be a gradual process with lamella slippage and breaking which triggers the β–α polymorphic transition.

1. Introduction

It is well known that the deformation-induced structure transitions in semicrystalline polymers can allow the manipulation of mechanical properties. Upon deformation, the isotropic structure of polymer materials can be transformed into an anisotropic structure due to the orientation of polymer chains. Hence, the mechanism of such transitions and how they are related to the resulting morphology, structure, and physicomechanical properties are of great scientific interest and practical importance in polymer science. It is also understood that when crystalline polymers are in the molten state, chains are entangled in a dynamic manner. As the temperature is reduced, some chains can crystallize and the entanglement points are excluded from the crystalline domains and become concentrated in the interlamellar amorphous regions. Thus, the concentration and distribution of chain entanglements in interlamellar amorphous regions would affect the final mechanical properties. The applicable properties of crystalline polymers are determined by their final formed structures and the process of structure formation. The mechanical properties of simecrystalline polymeric materials are also influenced by crystallinity, crystalline structure and morphology, amorphous chain orientation, distribution, and concentration of tie chains in the interlamellar amorphous regions. The processing and structure of crystalline polymers are attracting interests from researchers due to their promising performances. Polymer materials show a strong tendency to polymorphism presenting transitions from one polymorphic form to another. The appearance of one or other crystalline modification depends on many factors. These include crystallization conditions (melt or solution temperature, rate of cooling, presence of specific nucleating agents, type of substrate, etc.), mechanical treatment (drawing, pressing, rate of treatment, a. o.) [1–6].

Isotactic polypropylene (iPP) is one of the most important thermoplastic polymers owning to its low manufacturing cost and rather versatile properties. It is a typical polymorphic plastic with at least four basic crystalline forms: monoclinic (α), trigonal (β),

* Corresponding author.
E-mail address: scjiang@tju.edu.cn (S. Jiang).

0032-3861/$ – see front matter © 2012 Elsevier Ltd. All rights reserved.
doi:10.1016/j.polymer.2012.02.012

orthorhombic (γ) form, and smectic mesophase [7–9]. The monoclinic α phase is the dominating crystal modification when the polymer material solidifies from the meld under ordinary conditions. The β form is usually induced by flow or β-nucleating agents. Pure β-phase iPP can be obtained with the aid of crystalline nucleating agents. The γ form is preferentially formed from crystallization under pressure [10]. Under certain conditions, e.g. undercooling, a mesophase usually referred to as 'smectic' is formed instead of crystalline phase [11]. Varga reported differences in physical properties between α and β forms of iPP [12,13]. It has been demonstrated that the presence of β form crystal leads to enhanced toughness and ductility comparing to the higher modulus and tensile strength of α form. In general, excellent toughness is attributed to energy dissipation during yield process accompanied with structure transition from α to β form. The growth rate of β spherulites is up to 70% faster than that of spherulites. β-iPP is metastable relative to α-iPP, it has lower density (0.92 g/cm^3) [14] and is unstable upon stretching, which produces a transition to α-iPP or to the "smectic" form depending on whether the sample is processed above or below 60 °C. The impact strength and toughness of β-iPP exceed those of α-iPP. The improved mechanical performance of β-iPP makes it attractive for numerous applications [15,16].

The mechanical behavior of a semicrystalline polymer is believed to be strongly affected by the mechanical coupling or stress transmission between crystalline and amorphous structures [17–22]. Luo et al. demonstrated that the connection between crystallites might mainly determine the toughness of iPP instead of the β crystal form content [23]. The β–α transition can be triggered by mechanical loading [24]. The studies on deformation mechanism of β form iPP have indicated that interlamellar slippage and crazing development were the dominant modes for structure transformation. The improvement of mechanical properties during mechanical loading of β-iPP has been explained by the transition from β- to α-crystalline iPP (α-iPP), based principally on DSC experiments [1,2,25]. The metastable crystal structure can prevail under strained conditions because of the reduced entropy.

Recently, in-situ and ex-situ synchrotron X-ray, atomic forced microscopy (AFM) and optical microscopy (OM) techniques were carried out to investigate the deformation of polyolefin (including iPP and polyethylene, PE) by many researchers [26–31]. For example, Feng Zuo et al. studied deformation-induced structure changes during uniaxial stretching of iPP. Their results indicate that the dominant structure change is the transformation of folded-chain crystal lamella (monoclinic α-form) to oriented mesomorphic phase at room temperature and the dominant change is the transformation of amorphous phase to oriented folded-chain crystal lamella at high temperatures (>60 °C) [32]. Men et al. have focused on the formation and evolution of cavities in P1B during tensile stretching [33]. Yoshinobu Nozue et al. obtained the structure information on parent and daughter lamellae of iPP in various orientations during hot drawing [27]. Therefore, the deformation behavior is important to understand the properties of polymers [27,34]. Refer to iPP, there remains some uncertainty about the actual situation of β-iPP deformation and β–α transition due to inadequate experimental conditions. Some researchers got conclusions by studying stress damaged zone after tensile fracture [35,36] or the specimens which were subjected to drawing until neck formation at its failure [1]. Update synchrotron radiation X-ray microdiffraction has been employed to investigate the strain-induced crystalline modification in the plastic zone of an iPP β-phase [37–39]. These methods are not accurate enough to understand the actually change in the crystalline and amorphous phase with the development of the sample without consideration of temperature effects.

In this study, β nucleating agent aryl amide derivative (TMB-5) was doped to prepare β-PP for in-situ deformation study of β-iPP using combined synchrotron X-ray scattering methods. TMB-5 is a temperature dependent selective and efficient nucleating agent for iPP crystallization as shown in our previous study [40]. In-situ structural investigations on β-iPP transition during deformation at various temperatures were carried out with synchrotron SAXS and WAXS techniques. The temperature related critical strains for β form to α form transition of iPP were obtained. It is possible to understand the temperature related structure transition and deformation mechanism of β PP with uniaxial stretching and obtain the real relationship between the structure and properties.

2. Experimental section

2.1. Materials

The iPP used in this study is a commercial product of Aldrich Chemical Company, Inc. The *M*w and *M*n determined by gel permeation chromatography (GPC) were 339 869 and 74 492, respectively. The melting point of iPP is around 165 °C. The used β nucleating agent TMB-5 was supplied by Chemical Institute of Shanxi, China.

2.2. Sample preparation

iPP granules and TMB-5 powder were put into the 60 mL chamber of an XSS-300 torque rheometer together and melt-mixed at 190 °C for 10 min with a rotation speed of 30 rpm to prepare TMB-5 doped iPP samples. The concentrations of the nucleating agent were 0.05, 0.08, 0.1, 0.2, 0.5, and 1 wt%. Dumbbell-shaped sample bars with dimensions of 26.0 mm (length) × 1.5 mm (neck width) × 3 mm (neck length) were prepared.

2.3. Synchrotron SAXS and WAXS measurements

X-ray scattering experiments were performed using synchrotron radiation with λ = 0.154 nm at Beamline 4B9A of Beijing Synchrotron Radiation Facility (Beijing, China). Mar165-CCD was set at 1606 mm and 168 mm sample-detector distance in the direction of the beam for SAXS and WAXS data collections, respectively.

2.4. Tensile measurements

Uniaxial tensile deformation experiments were performed using a Linkam TST-350 tensile hot stage (Linkam Scientific Instruments, Ltd., U.K.), which stretched the sample bar symmetrically. The symmetric stretching ensured that the focused X-ray beam could illuminate the same sample position during deformation. The stage can be designed to apply two kinds of tensile modes: constant rate and constant force within a wide range of tensile rates and strains. The mechanical design and electronics of the Linkam tensile hot stage provided a precise control of the parameters for the tensile experiment that included temperature, heating/cooling rates, and sample thickness. The deformation measurements were carried out at 30 °C, 60 °C, 80 °C, 100 °C and 120 °C. As the temperature reached the target value at a rate of 30 °C/min, a constant deformation rate of 10 μm/s was applied to the samples. Then the sample was kept at the fixed temperature until fracture and the structure information was recorded by WAXS or SAXS simultaneously. The Linksys 32 software was used to collect and analyze the tensile data. The stress and strain mentioned in this study are all engineering stress and engineering strain obtained from the tensile hot stage.

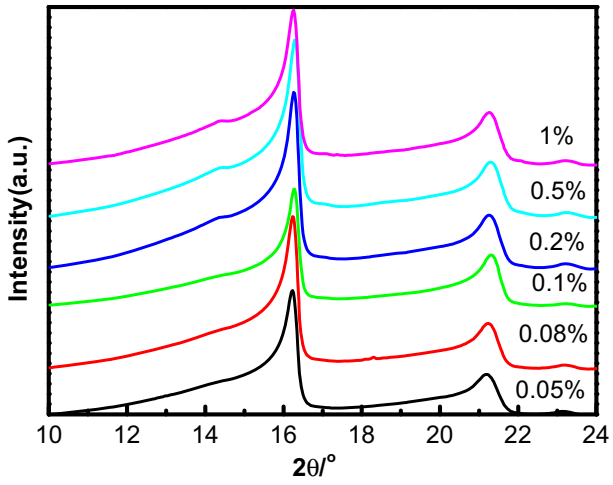

Fig. 1. WAXS profiles of nucleated iPP with different TMB-5 contents taken along the meridional direction before drawing at 100 °C.

3. Results and discussion

TMB-5 doped iPP with different proportions were used to prepare β-PP. Fig. 1 shows the WAXS profiles of prepare β-PP. The structure analysis on obtained data indicates that the amount of nucleating agent in the TMB-5 doped iPP is not so important to form the content of β-PP, because TMB-5 is an efficient nucleating agent for iPP crystallization. Therefore, one of the samples with fixed TMB-5 content was carried out for the measurements and investigations. The engineering stress–strain curve of β-PP during uniaxial tensile deformation at 30 °C, together with selected 2D WAXS and SAXS patterns collected at several selected points on behalf of mechanical property changes (the point before stretching, yield point, the transition point from strain softening to strain hardening and points during strain hardening) are shown in Fig. 2. The stress–strain curve of β-PP indicates that it is a typical ductile fracture with obvious elastic stage, yield point, strain softening and strain hardening. A yield point can be found from the curve soon after deformation began, at a strain of 5%. The subsequent stress dropped rapidly and then increased with strain, which corresponding to the dominant process of strain hardening stage.

Micro- and meso-scale structure evolutions were analyzed according to the obtained WAXS and SAXS patterns during the uniaxial stretching of β-PP. The changes of long spacing were obtained from the equatorial (perpendicular to the tensile direction) scattering according to SAXS analysis, and the meridional (parallel to the tensile direction) streak that might be tainted with the occurrence of micro-voids [41–43]. As shown in Fig. 2, the 2D SAXS and WAXS patterns imply that the orientation is not obvious for the sample without stretching and two diffraction rings could be detected by 2D WAXS. The diffraction rings correspond to (300) and (301) (from inner to outer) of typical β-form iPP diffraction. The corresponding SAXS pattern indicates the negligible orientation of lamellar structure. From the results in Fig. 2, it can be found that the

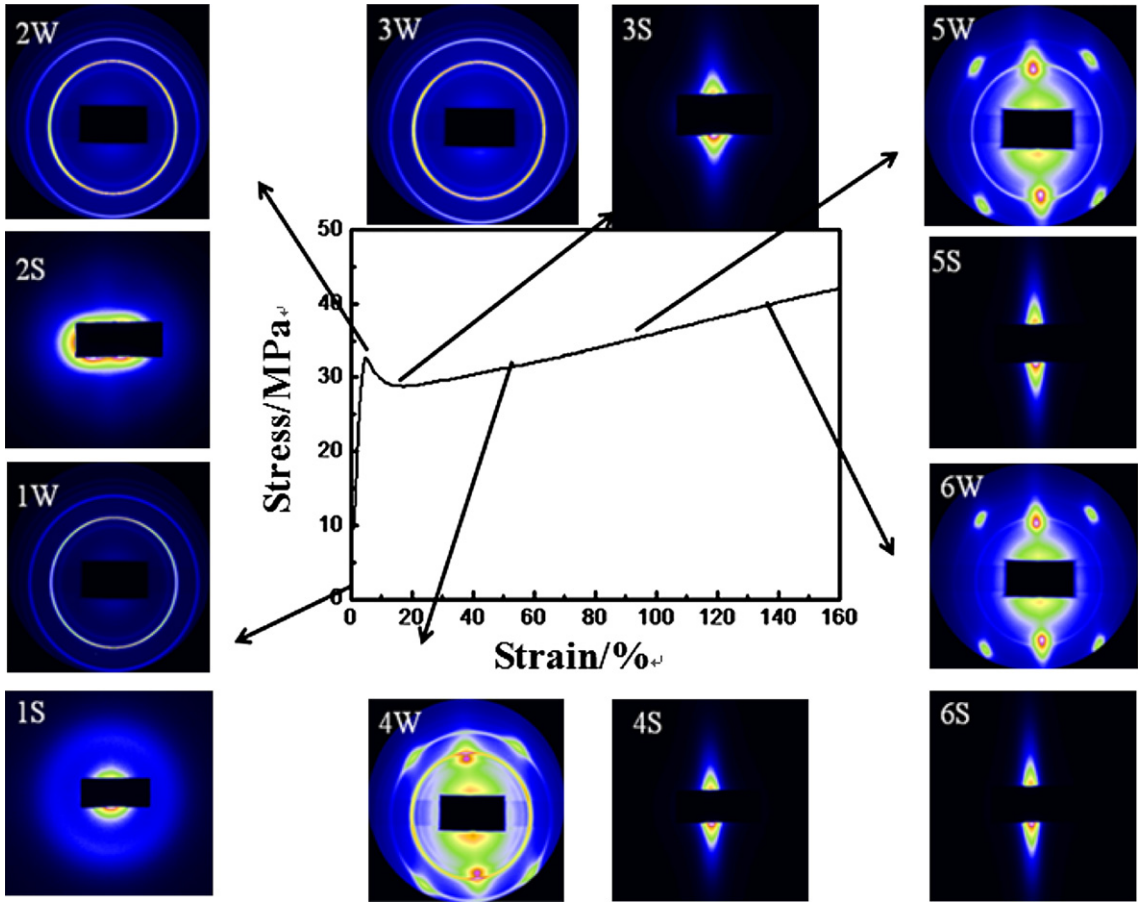

Fig. 2. Engineering stress–strain curve and selected 2D SAXS and WAXS patterns acquired during uniaxial tensile deformation of iPP/TMB-5(TMB/iPP = 0.5%) blends at room temperature (30 °C) (the sample was stretched in horizontal direction).

related 2D WAXS and 2D SAXS patterns changed dramatically after the yield point. In addition, 2D SAXS patterns obtained after the yield point are not typical scattering patterns. At the same time, the orientation can be clearly observed from of all diffraction rings as shown in 2D WAXS patterns during strain hardening stage.

The scattering intensity profiles as indicated taken along the meridional direction and the equatorial direction from 2D WAXS and SAXS patterns at different strain extracted from Fig. 2 are illustrated in Fig. 3. Both SAXS and WAXS results in Fig. 3 indicate obvious change of scattering curves before and after the yield point. Typical diffraction can be found for β PP without deformation as shown in Fig. 3A and B. Upon deformation, the intensity of the diffraction peaks decreased. Such a behavior, especially the decreasing intensity in the (300) reflection of WAXS, suggested that selective melting and rearranging of the residual structure took place [32]. At strain = 42%, an abrupt change of the diffraction related to the crystalline structure can be seen, as confirmed by the diffraction peak of (300) trend to convert to (110) diffraction peak which corresponds β–α transition. It implied that the β–α transformation during mechanical loading was not completed even in the process zone at 30 °C. The β–α transformation is associated with micro-voiding [36], the light scatter among these micro-voids within the plastic zone is responsible for the 'whitening' effect, usually termed to 'stress whitening'. The formation of micro-voids during the phase transformation results in a characteristic SAXS pattern which overlays the SAXS pattern of β-iPP. This phenomenon has more pronounced effect at low temperature. So the projected scattering intensity is very weak above strain 10% for SAXS profiles. At the later stage of deformation as shown in Fig. 2, the SAXS pattern exhibited a strong meridional streak, consistent with formation of micro-voids and strain-induced crystalline fibrils that would occur when the stretched β-iPP sample bars fractured at strain 160%.

Uniaxial tensile induced deformation of β-iPP films was also carried out at various temperatures. The engineering stress–strain curve and selected 2D WAXS and SAXS patterns obtained at 120 °C are illustrated in Fig. 4. Similar to the deformation at 30 °C, there was a yield point at strain 7% for deformation at 120 °C. Under this condition, the degree of strain hardening was significantly larger than those at 30 °C. Furthermore, the stress at yield point for deformation at 120 °C is below that at 30 °C (9 and 32.7 MPa, respectively). The obtained engineering stress–strain curve is generally similar to that obtained at 30 °C. However, distinct differences of related structure could be found. As shown in Fig. 4, the initial obtained SAXS pattern became two-bar like above the yield point, indicating that stacks became aligned perpendicularly to the stretching direction. The two-bar SAXS pattern on the equator projected scattering intensity can be explained by the following events [32,44]: (i) a fraction of lamellar stacks that were parallel (or partially parallel) to the stretching direction were reoriented due to the tendency of chain orientation with stretching; (ii) a fraction of lamellar stacks that were perpendicular (or partially perpendicular) to the stretching direction became fragmented due to the chain pulling-out mechanism. 1D WAXS profiles along two directions extracted from Fig. 4 are illustrated in Fig. 5A and B. It can be found that the structure transformation of β–α crystal occurred at a much lower strain than that at 30 °C, evidenced by the appearance of the (110) peak on the meridian. As shown in Fig. 3, the transition occurred at a strain of about 42.5% at 30 °C, while the change took place at a strain of about14.8% at 120 °C. It was interesting to note that the β–α transformation was obvious during deformation, where three distinct diffraction peaks

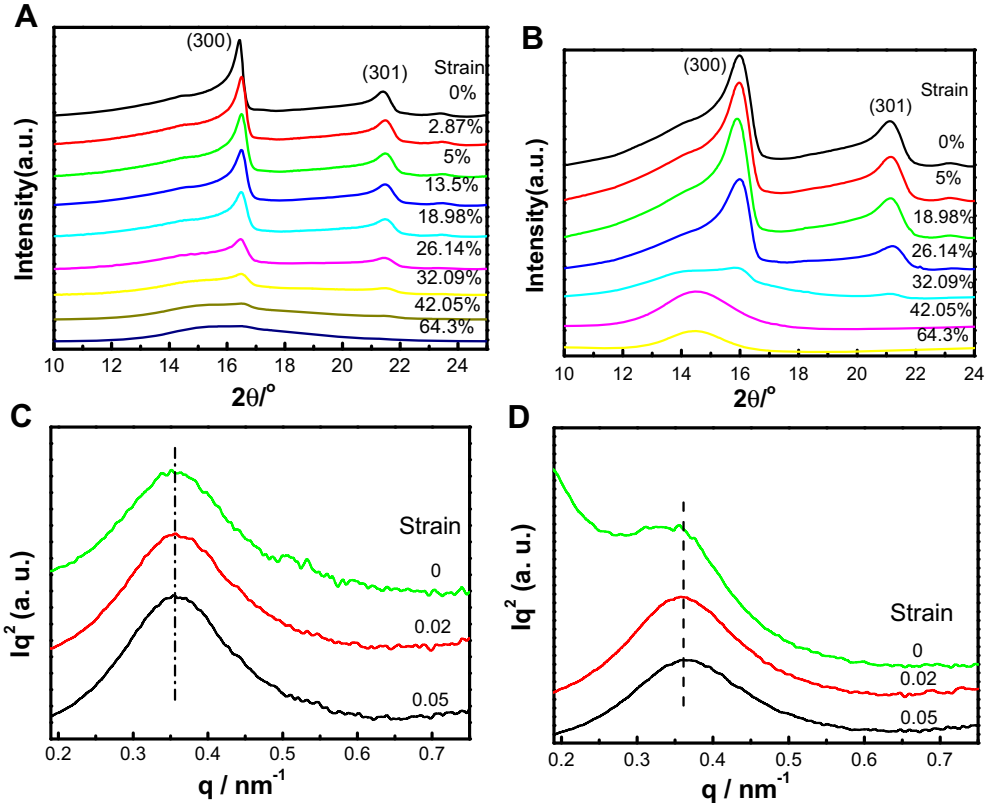

Fig. 3. 1D WAXS profiles along (A) the meridional direction and (B) the equatorial direction and projected linear SAXS intensity profiles (Iq^2 vs q) along (C) the meridional direction and (D) the equatorial direction at different strains corresponding to Fig. 2.

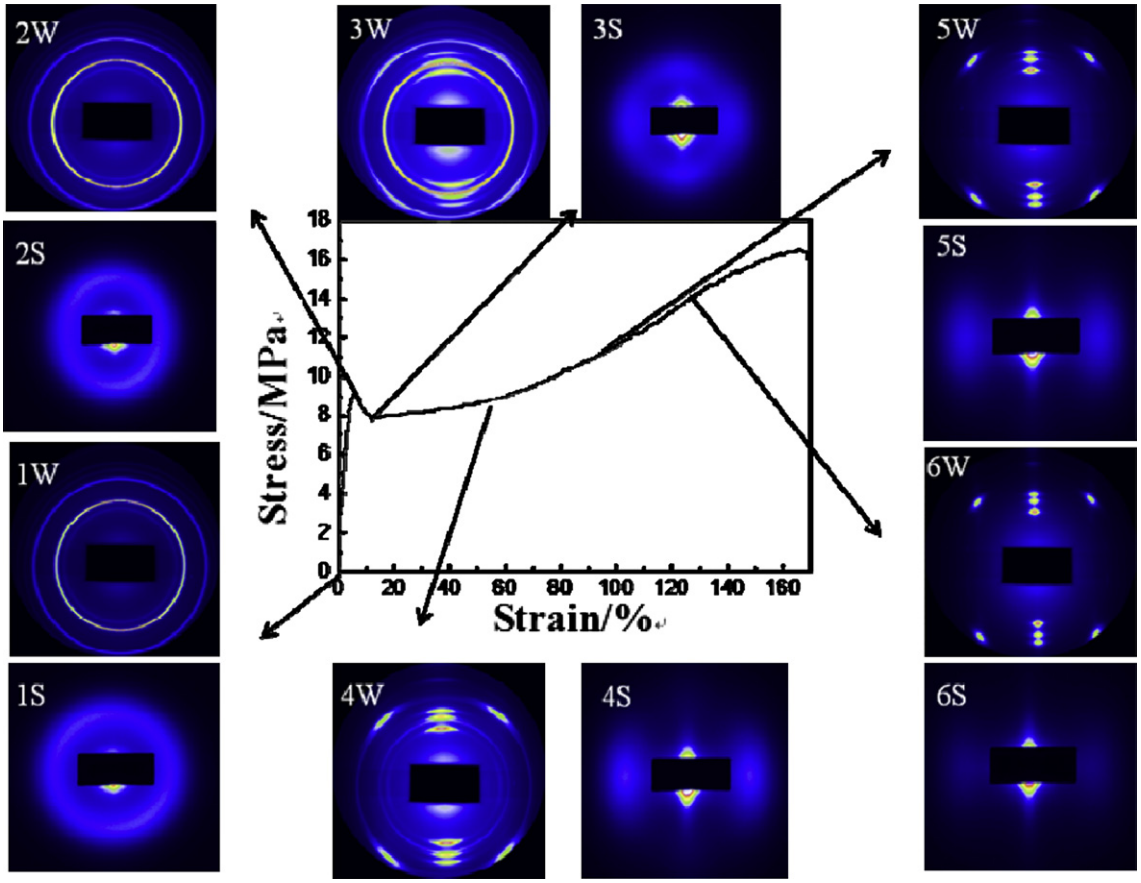

Fig. 4. Engineering stress–strain curve and selected 2D SAXS and WAXS patterns acquired during uniaxial tensile deformation of iPP/TMB-5(TMB/iPP = 0.5%) blends at 120 °C (the sample was stretched in horizontal direction).

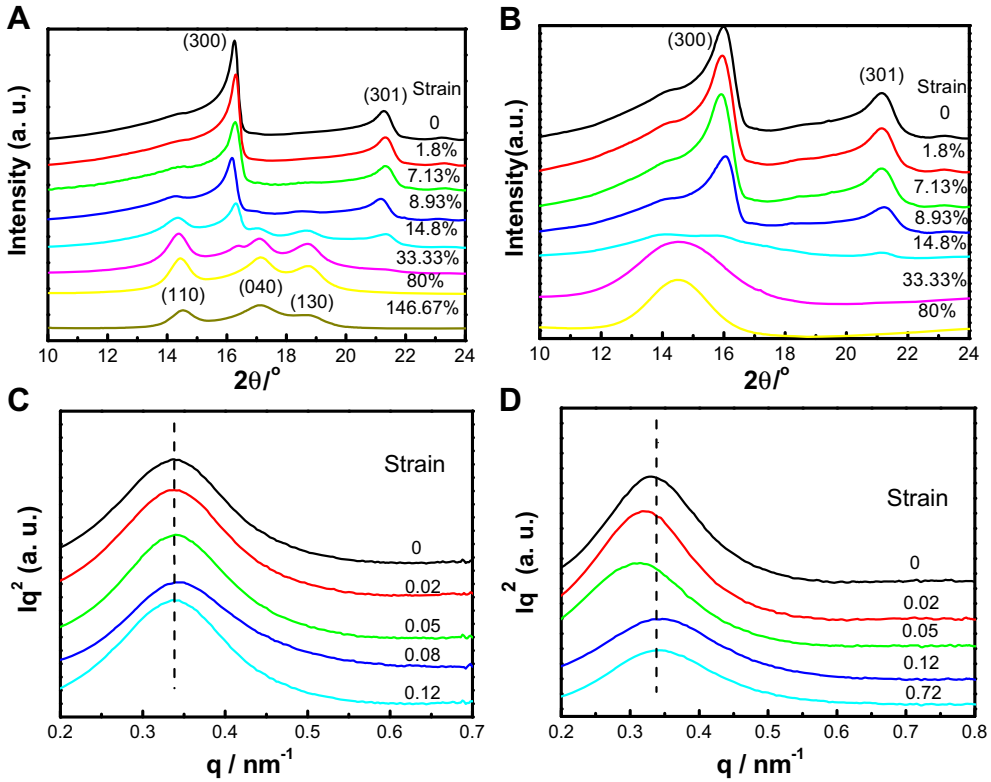

Fig. 5. 1D WAXS profiles along (A) the meridional direction and (B) the equatorial direction and projected linear SAXS intensity profiles (Iq^2 vs q) along (C) the meridional direction and (D) the equatorial direction at different strains corresponding to Fig. 4.

((110), (040) and (130)) could be seen even at a high strain of 80% before breaking, which imply that higher temperature promoted the conduct of the β–α transformation. It has been reported that the transformation from unstable β-PP to stable α-PP for iPP can be achieved through two different processes. One is the partial melting and recrystallization processes during the heating and/or annealing treatment at a certain temperature and the other is the solid to solid martensitic-like transformation. For long time the postulated β–α martensitic transformation seemed problematic since it would require reversal of helical handedness, which was considered impossible in solid [45]. The 1D SAXS profiles taken along the two directions of the 2D SAXS patterns are shown in Fig. 5C and D. Unexpected results can be found in the Fig. 5D that the position of the scattering peak shifted to a lower q value with stretching, then it shifted to near the original position with further stretching.

In order to understand the interesting phenomena obtained at 120 °C, the measurements at 60 °C, 80 °C, 100 °C and further analysis of the obtained results have been done. It is known that the changes in samples during tensile deformation occurred mainly among crystalline, amorphous and mesomorphic phase [13,32,39,44]. The correlated temperature and strain of β–α transformation would be helpful to understand the relationship between the structure and properties of investigated samples. It would be benefit to know the mechanism of β–α transformation of β PP under uniaxial stretching.

The long period of investigated samples was estimated from the projected scattering peak position of the Iq^2 vs q plot ($L = 2\pi/q_{max}$) [46]. The strain related long period during uniaxial tensile deformation at 120 °C of iPP/TMB-5(TMB/iPP = 0.5%) blends along the meridional direction (A) and the equatorial direction (B) are showed in Fig. 6. The estimated long period at 120 °C before deformation was 20.6 nm. Because of cavitations during sample stretching, we had to observe the long period before the yield point in meridional direction. The formation of cavitations during the phase transformation overlaid the SAXS pattern of β-iPP after the yield point. Fig. 6B shows that the long period along the equatorial direction increased obviously from 20.6 to 24.7 nm between strain 0 and 6.93% and then decreased from 24.7 to 20.2 nm between strain 6.93% and 23.53%. Above strain 23.53%, the long period remained almost constant within the observed range. Corresponding to the engineering stress–strain curves, it was found that the long period increased with strain in the elastic deformation stage before the yield point, then the long period decreased rapidly until it reached a stable value after the yield point. As mentioned above, the changes in the elastic deformation stage before yield point occurred in amorphous region or mesomorphic phase. In general, the chains in the amorphous region could be oriented along the tensile direction when the sample is stretched. The sample size increases with stretching in this direction, while the sample size reduces in the direction perpendicular to the stretching. Therefore, the long period parallel to the tensile direction should be increased and the long period perpendicular to the tensile direction should be reduced. However, the results in Fig. 6 are conflicted with the common knowledge of stretched crystalline polymers. One can see from the results in Fig. 6 that the long period which perpendicular to the tensile direction before yield point increased and the long period along the tensile direction was almost the same. Benjamin S. Hsiao et al. [32,44] also observed the similar phenomenon in the deformation study of iPP with α form crystal and PPDL. They considered it could be attributed to the elastic deformation.

The phenomenon above mentioned could be understood as auxetic behavior. Negative poisson ratio is the character of auxetic behavior. In other words, the sample would become fatter when uniaxially stretched and thinner when uniaxially compressed. The phenomenon may result in various enhanced properties that include high-energy absorption properties, increased indentation resistance and so on [41]. The basic structural characteristic of the auxetic material is hinged chain structure which is opened during tensile; stretching of such a system in particular directions will result in a relative rotation of the lamellae. This may result in a more open structure, if one assumes that the different-sized lamellae are perfectly rigid and connected to each other through simple hinges, which only permit relative rotation of the lamellae. In the case of rotating squares, Poisson's ratio of the auxetic material is a negative value, irrespective of the direction of loading and dimensions of the squares.

The parent and daughter lamellae structure of iPP match the essential requirement of auxetic materials. The reports [15,16,47–49] have proved that there is a special parent-daughter lamella structure in iPP with highly oriented α crystal; daughter lamella epitaxial growth on the parent lamella, the angle is 80° or 100°. Auxetic behavior with negative Poisson's ratio was observed during a uniaxial tensile test. In-situ wide-angle and small-angle X-ray scattering measurements revealed that a relative rotation of parent and daughter lamella was accompanied with the expansion of sample width. During the tensile test, the angle between parent and daughter lamella rotates from initial 80° or 100° to close to 90°, which well accounts for the lateral expansion of the samples. The results demonstrate the mechanism based on special

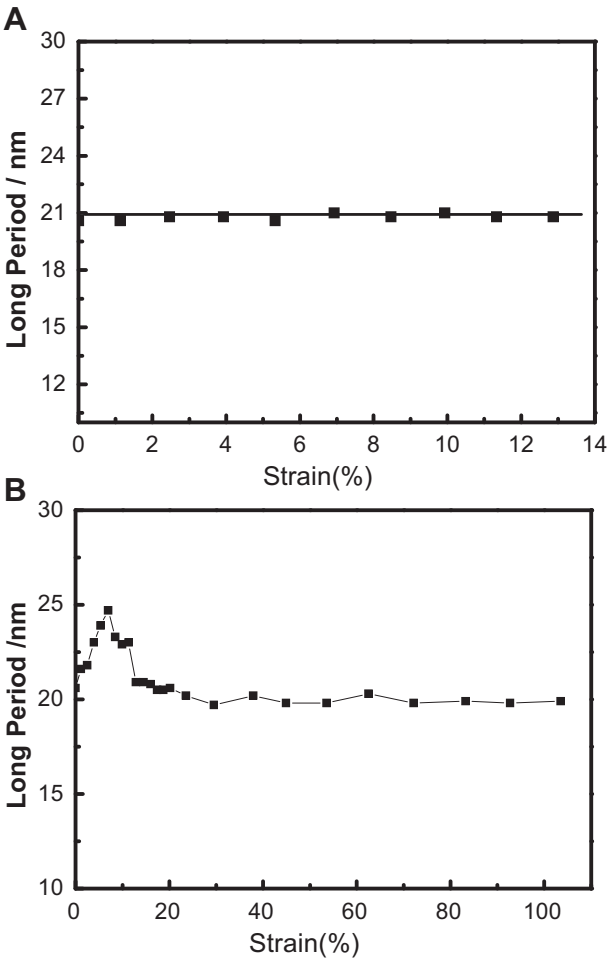

Fig. 6. The changes of the long period as a function of strain along the meridional direction (A) and the equatorial direction (B) corresponding to Fig. 5C and D.

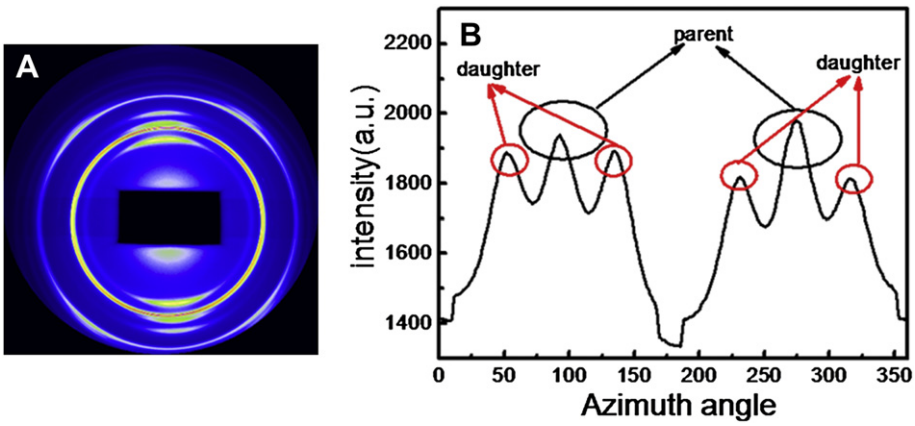

Fig. 7. (A) 2D WAXS patterns acquired during uniaxial tensile deformation at strain 17% of iPP/TMB-5(TMB/iPP = 0.5%) blends at 120 °C and (B) corresponding azimuthal spreads of the (300) reflection peak.

crystallography to design auxetic materials on a mesoscopic scale. The relative rotation of parent and daughter lamellae structure play an important role in formation of the micro-voids.

Based on the above discussions, we speculated that iPP with highly oriented β crystal constitute parent-daughter lamella structures. To clarify this issue, we conducted a similar data analysis according to the literature [47]. Because the parent and daughter lamella structure cannot be observed under quiescent condition, we analyzed the data during uniaxial tensile deformation. Fig. 7A and B are 2D WAXS patterns acquired during uniaxial tensile deformation at strain 17% of iPP/TMB-5 (TMB/iPP = 0.5%) blends at 120 °C and corresponding azimuthal spreads of the (300) reflection peak. From Fig. 7B we could see six diffraction peaks. According to the literature [47], we considered that the two diffraction peaks which were marked by black circle represent the parent crystals, while the other four diffraction peaks which were marked by red circle represent the daughter crystals. The azimuthal angle differences between daughter and parent crystallite from a group of parent-daughter crystallite structure corresponding to Fig. 7 is showed in Fig. 8. The result in Fig. 8 indicates that the angle between parent and daughter crystallite is about 40° or 140°. Therefore, the parent and daughter crystallite structure of iPP with highly oriented β crystal matches the essential requirement of auxetic behavior. During tensile, the angle between parent and daughter crystallite rotates from initial 40° or 140° to close to 90°, which well accounts for the lateral expansion of the samples. This is the reason for the long period increased with strain in the elastic deformation stage before the yield point along the equatorial direction. Then after yield point, the angle between parent and daughter crystallite deviates from 90° during the tensile which provides an explanation for the decrease in the long period. Initially, the oriented mesomorphic phase formed simultaneously with orientation of crystals. Then the mesomorphic phase partly transformed into oriented crystal phase with further deformation. Since transformation of the amorphous phase to oriented mesomorphic phase leads to a large reduction in entropy, this can also explain the phenomenon of long period decrease to the value which less than the initial value after the yield point (in Fig. 6B) [44].

Hernandez et al investigated the effects of strain-induced crystallization on the segmental dynamics of vulcanized natural rubber [50]. The strain-induced crystals developed and shorter

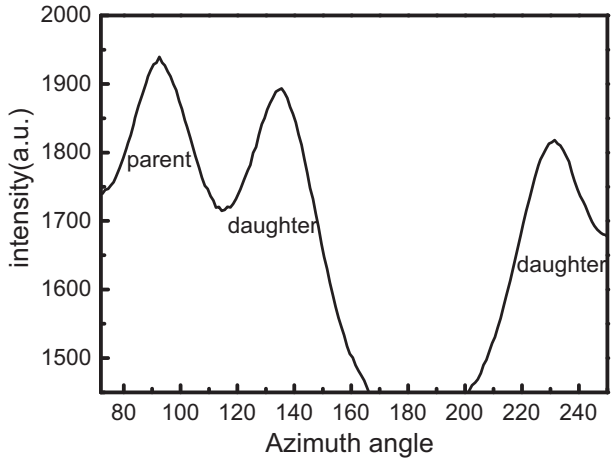

Fig. 8. Azimuthal angle differences between daughter and parent lamella from a group of parent-daughter lamella structure corresponding to Fig. 7.

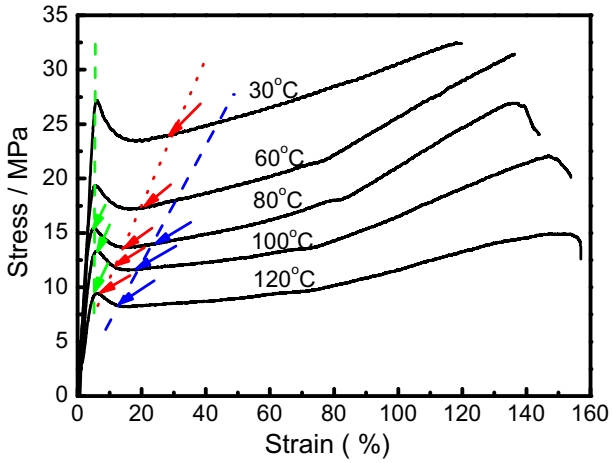

Fig. 9. The typical engineering stress–strain curves of iPP/TMB-5 (TMB/iPP = 0.5%) blends during uniaxial tensile deformation at different temperature (red arrow indicated initial of β–α transformation, green arrow indicated the max value of long period, blue arrow indicated the first point whose long period less than the initial value). (For interpretation of the references to color in this figure legend, the reader is referred to the web version of this article.)

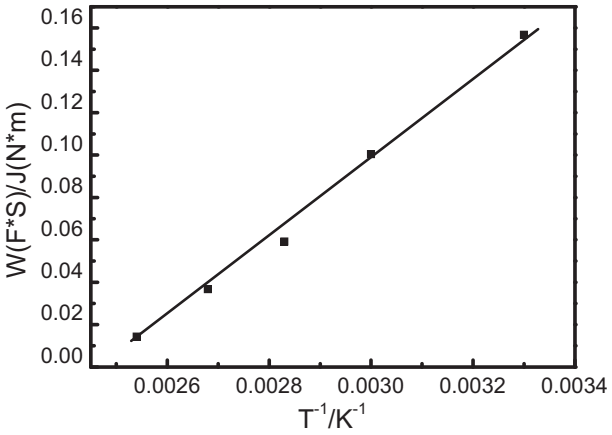

Fig. 10. A quantitative relationship between the mechanical work (force*distance) and the temperature of iPP/TMB-5(TMB/iPP = 0.2%) blends during uniaxial tensile deformation.

chains were progressively incorporated into the crystals. We considered that new crystalline lamella emerges and develops between two original lamellae which perpendicular to the tensile direction during the elastic deformation stage. The insertion of new lamella counteracts the increment in average distance (parallel to the tensile direction) between the adjacent lamellae provoked by stretching. Therefore, the long period along the tensile direction is almost constant. Moreover, the dimensions of the dumbbell-shaped sample bars is 26.0 mm (length) × 1.0 mm (neck width) × 3 mm (neck length). In the neck zone, the length is three times of the width which represents the numbers of chains along the meridional direction is three times of the numbers along the equatorial direction. So the changes of long period along the equatorial direction should be more obvious than the changes along the meridional direction. This is why the long period that perpendicular to the tensile direction increases in the elastic deformation stage (Fig. 6B) and the long period along the tensile direction is almost the same (Fig. 6A).

The engineering stress–strain curves of iPP/TMB-5 (TMB/iPP = 0.5%) blends together with structure regions in the stress–strain curves according to the analysis of SAXS and WAXS data obtained at different temperatures (30 °C, 60 °C, 80 °C, 100 °C, 120 °C) are shown in Fig. 9. The red arrows and red dot line relate to the initial of β–α transformation; the green arrows and green dash line correspond to the max value of long period; the blue arrows and blue dash line involve the first point that the long period are less than the initial value during the deformation. From the results in Fig. 9, we can see that the max values of long period are located near the yield points which represents the angle between parent

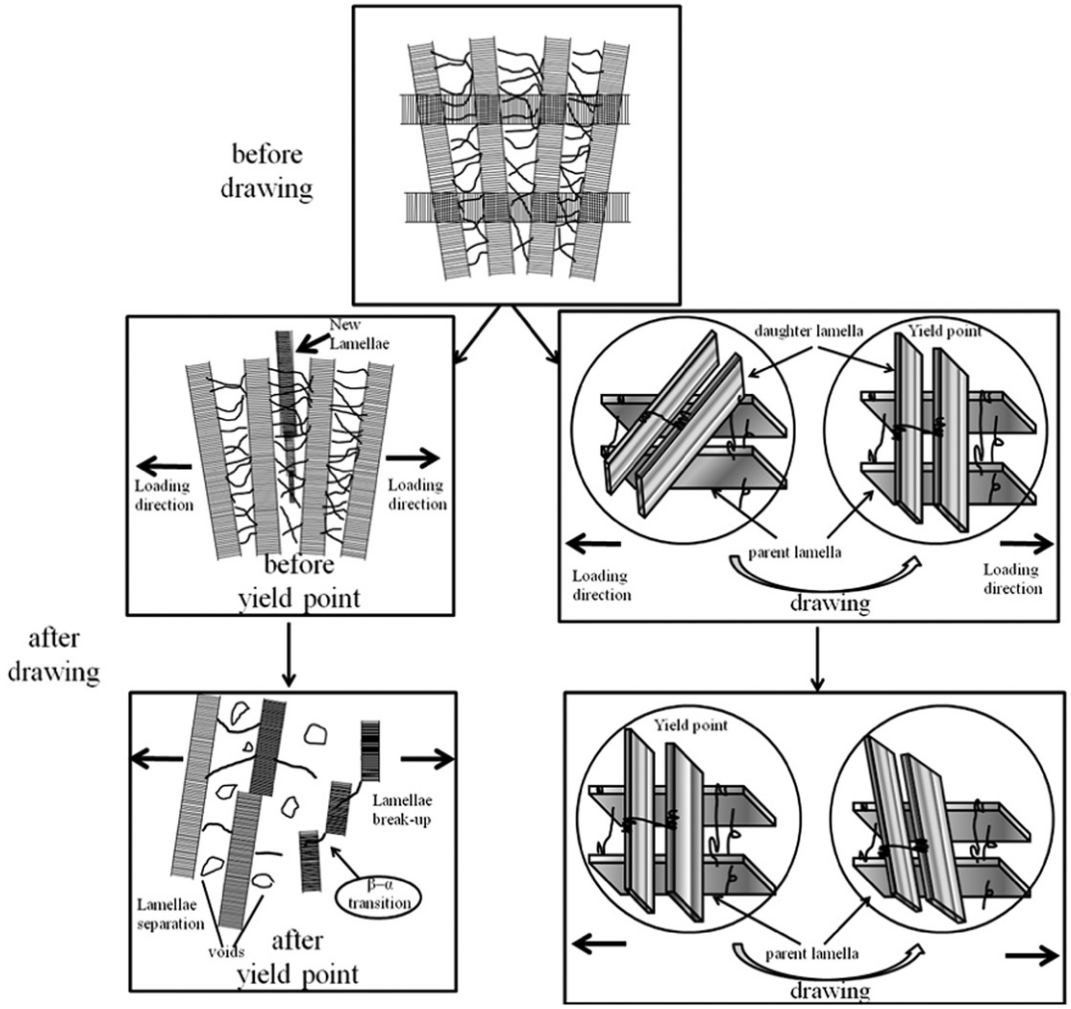

Fig. 11. Schematic mechanism for the transitions of the crystal and amorphous phases in β PP during uniaxial tensile deformation before and after yield point.

and daughter lamellae close to 90° near the yield point. The initial stain of strain-induced β–α transformation decreases with the tensile temperature. The first points where long-periods in the stress–strain curves are less than the initial value decrease with the tensile temperature. The changes in the crystalline form began after the yield point; while the changes in the elastic deformation stage before yield point mainly occurred in amorphous phase or mesomorphic phase.

The results in Fig. 9 suggest that the initial strain of the crystal transformation decreases as the temperature rises. In other words, when the transition occurred between different crystals, the tensile displacement of the sample reduced. One can find that the tensile force also decreased in the figure. The equation, $W = F \times S$, (where W is mechanical work, F is force, S is displacement), would be helpful to understand the relationship between the temperature dependent crystalline structure transition and the energy required for the transition. The mechanical work required for promoting crystal transition of the sample decreases with temperature increasing. We speculated that a quantitative relationship exists between the mechanical work and the temperature. Fig. 10 is 1/T vs $F \times S$ plot of iPP/TMB-5 (TMB/iPP = 0.2%) blends during uniaxial tensile induced deformation. It proved that there was a linear relationship between 1/T and mechanical work (force × distance). According to data analysis, iPP/TMB-5 blends of other proportions have the similar relationship. We consider it is an open problem to understand the deformation behavior of semicrystalline polymers.

A schematic mechanism is shown in Fig. 11 to illustrate the deformation and transition process of β PP during uniaxial tensile before and after yield point. In the elastic deformation stage before yield point, there are two processes occur simultaneously. One is new crystalline lamella emerges and develops between two original lamellae which perpendicular to the tensile direction. The insertion of new lamella counteracts the increment in average distance (parallel to the tensile direction) between the adjacent lamellae provoked by stretching. The other is the angle between parent and daughter lamellae rotates from initial 40° or 140° to close to 90° during the stretching between lamellae that parent lamella parallel to the tensile direction, which well accounts for the lateral expansion of the samples. After yield point, the mechanical loading-induced β–α transition seems to be a gradual process, lamellae begin to slippage and break-up which triggers the β–α polymorphic transition. In the amorphous regions, the angle between parent and daughter lamellae deviates from 90° during the tensile test.

4. Conclusions

From the deformation and structure transitions study of iPP/TMB-5(TMB/iPP = 0.5%) blends stretched at different temperatures (30, 60, 80, 100 and 120 °C), a quantitative relationship exists between the mechanical work and the temperature was obtained. The WAXS data indicates that the β–α transformation is more obvious at higher temperature (120 °C) than that at room temperature during tensile deformation, which showed that temperature promoted the conduct of the β–α transformation. The analysis of SAXS data indicated that the long period increases with strain in the elastic deformation stage before the yield point along the equatorial direction, while the long period along the tensile direction is almost keeping constant. iPP with highly oriented β crystal constructed with parent-daughter lamellae structures which matches the essential requirement of auxetic behavior. The angle between parent and daughter crystallite is about 40° or 140°. The angle between parent and daughter lamella rotates from initial 40° or 140° to close to 90° during stretching, which well accounts for the lateral expansion of the samples.

Acknowledgment

This work was supported by National Natural Science Foundation of China (51173130, 20974077, 50903061).

References

[1] Boyanova M, Calleja FJB, Fakirov S. J Mater Sci 2006;41:5504–9.
[2] Ran SF, Zong XS, Fang DF, Hsiao BS, Chu B. Macromolecules 2001;34:2569–78.
[3] Jerabek M, Major Z, Renner K, Móczó J, Pukánszky B, Lang RW. Polymer 2010;51:2040–8.
[4] Liu JP, He YN, Wang XG. Polymer 2010;51:2879–86.
[5] Hossain D, Tschopp MA, Ward DK, Bouvard JL, Wang P, Horstemeyer MF. Polymer 2010;51:6071–83.
[6] Ube T, Aoki H, Ito S, Horinaka J, Takigawa T, Masuda T. Polymer 2009;50:3016–21.
[7] Liu MX, Guo BC, Du ML, Chen F, Jia DM. Polymer 2009;50:3022–30.
[8] Menyhárd A, Gahleitner M, Varga J, Bernreitner K, Jääskeläinen P, Øysæd H, et al. Eur Polym J 2009;45:3138–48.
[9] Zhang PY, Liu XX, Li YQ. Mater Sci Eng A 2006;434:310–3.
[10] Hoyos M, Tiemblo P, Gómez-Elvira JM. Eur Polym J 2009;45:1322–7.
[11] Lezak E, Bartczak Z, Galeski A. Polymer 2006;47:8562–74.
[12] Chen HB, Karger-Kocsis J, Wu JS, Varga J. Polymer 2002;43:6505–14.
[13] Varga J. J Macromol Sci Phys 2002;41:1121–71.
[14] Li JX, Cheung WL. Polymer 1999;40:2085–8.
[15] Shangguan YG, Song YH, Peng M, Li BP, Zheng Q. Eur Polym J 2005;41:1766–71.
[16] Han L, Li XX, Li YL, Huang T, Wang Y, Wu J, et al. Mater Sci Eng A 2010;527:3176–85.
[17] Seguela R. Macromol Mater Eng 2007;292:235–44.
[18] Humbert S, Lame O, Vigier G. Polymer 2009;50:3755–61.
[19] Humbert S, Lame O, Chenal JM, Rochas C, Vigier G. Macromolecules 2010;43:7212–21.
[20] Van-Pham DT, Sorioka K, Norisuye T, Tran-Cong-Miyata Q. Polymer 2011;52:739–45.
[21] Galeski A, Bartczak Z, Kazmierczak T, Slouf M. Polymer 2010;51:5780–7.
[22] Liu GM, Guan Y, Wen T, Wang XW, Zhang XQ, Wang DJ, et al. Polymer 2011;52:5221–30.
[23] Luo F, Geng CG, Wang K, Deng H, Chen F, Fu Q, et al. Macromolecules 2009;42:9325–31.
[24] Karger-Kocsis J. Polym Eng Sci 1996;36:203–10.
[25] Riekela C, Karger-Kocsis J. Polymer 1999;40:541–5.
[26] Song Y, Nitta K, Nemoto N. Macromolecules 2003;36:1955–61.
[27] Nozue Y, Shinohara Y, Ogawa Y, Sakurai T, Hori H, Kasahara T, et al. Macromolecules 2007;40:2036–45.
[28] Koike Y, Cakmak M. Macromolecules 2004;37:2171–81.
[29] Hong K, Strobl G. Macromolecules 2006;39:268–73.
[30] Koike Y, Cakmak M. J Polym Sci B Polym Phys 2006;44:925–41.
[31] Nozue Y, Shinohara Y, Ogawa Y, Takamizawa T, Sakurai T, Kasahara T, et al. Polymer 2010;51:222–31.
[32] Zuo F, Keum JK, Chen XM, Hsiao BS, Chen HY, Lai SY, et al. Polymer 2007;48:6867–80.
[33] Men YF, Rieger J. Macromolecules 2004;37:9481–8.
[34] Abbassi-Sourki F, Huneault MA, Bousmina M. Polymer 2009;50:645–53.
[35] Krumova M, Karger-Kocsis J, Calleja FJB, Fakirov SJ. Mater Sci 1999;34:2371–5.
[36] Karger-Kocsis J, Shang PP. J Therm Anal 1998;51:237–44.
[37] Pawlak A, Galeski A. Macromolecules 2005;38:9688–97.
[38] Zuo F, Mao YM, Yi XW, Burger C, Hsiao BS. Macromolecules 2011;44:3670–3.
[39] Rozanski A, Galeski A, Debowska M. Macromolecules 2011;44:20–8.
[40] Cai Z W, Zhang Y, Li JQ, Shang YR, Huo H, Feng JC, et al. Unpublished.
[41] Wu J. Polymer 2003;44:8033–40.
[42] Aerts J. J Appl Crystallogr 1991;24:709–11.
[43] Wu J, Schultz JM, Yeh F, Hsiao BS, Chu B. Macromolecules 2000;33:1765–77.
[44] Cai AL, Hsiao BS, Gross RA. Macromolecules 2011;44:3874–83.
[45] Li XX, Wu YW, Bai HW, Liu L, Huang T. Mater Sci Eng A 2010;527:531–8.
[46] Hsiao BS, Kennedy AD, Leach RA, Chu B, Harney P. J Appl Crystallogr 1997;30:1084.
[47] Bai LG, Wang DL, Li LB, Pan GQ, Li XH. J Univ Sci Technol 2010;40:618–22.
[48] Li HH, Sun XL, Yan SK, Schultz JM. Macromolecules 2008;41:5062–4.
[49] Li HH, Zhang XQ, Duan YX, Wang DJ, Li L, Yan SK. Polymer 2004;45:8059–65.
[50] Hernandez M, Lopez-Manchado MA, Sanz A, Nogales A, Ezquerra TA. Macromolecules 2011;44:6574–80.